Published in final edited form as:
Dev Biol. 2012 December 15; 372(2): 263–273. doi:10.1016/j.ydbio.2012.09.021.

BMP2 induces segment-specific skeletal regeneration from digit and limb amputations by establishing a new endochondral ossification center

Ling Yu[1], **Manjong Han**[1], **Mingquan Yan**[1], **Jangwoo Lee**[1,3], and **Ken Muneoka**[1,2,§]

[1]Division of Developmental Biology, Department of Cell and Molecular Biology, Tulane University, New Orleans, LA 70118, USA

[2]Center for Bioenvironmental Research, Tulane University, New Orleans, LA 70118, USA

Abstract

Bone morphogenetic proteins (BMPs) are required for bone development, the repair of damage skeletal tissue, and the regeneration of the mouse digit tip. Previously we showed that BMP treatment can induce a regeneration response in mouse digits amputated at a proximal level of the terminal phalangeal element (P3) (Yu et al., 2010). In this study, we show that the regeneration-inductive ability of BMP2 extends to amputations at the level of the second phalangeal element (P2) of neonatal digits, and the hindlimb of adult limbs. In these models the induced regenerative response is restricted in a segment-specific manner, thus amputated skeletal elements regenerate distally patterned skeletal structures but does not form joints or more distal skeletal elements. Studies on P2 amputations indicate that BMP2-induced regeneration is associated with a localized proliferative response and the transient expression of established digit blastema marker genes. This is followed by the formation of a new endochondral ossification center at the distal end of the bone stump. The endochondral ossification center contains proliferating chondrocytes that establish a distal proliferative zone and differentiate proximally into hypertrophic chondrocytes. Skeletal regeneration occurs from proximal to distal with the appearance of osteoblasts that differentiate in continuity with the amputated stump. Using the polarity of the endochondral ossification centers induced by BMP2 at two different amputation levels, we show that BMP2 activates a level-dependent regenerative response indicative of a positional information network. In summary, our studies provide evidence that BMP2 induces the regeneration of mammalian limb structures by stimulating a new endochondral ossification center that utilizes an existing network of positional information to regulate patterning during skeletal regeneration.

Keywords

Skeletal regeneration; Endochondral ossification; BMP2; Digit; Limb; Positional Information; Mouse

[§]Author for correspondence: Ken Muneoka, Department of Cell & Molecular Biology, 2000 Percival Stern Hall, Tulane University, 504 865-5059, FAX 504 865-6785, kmuneoka@tulane.edu.
[3]Current Address: Department of Developmental and Cell Biology, University of California, Irvine, CA 92697-1450

Introduction

In mammals, the induction of a regenerative response from a non-regenerating amputation wound is a major goal of regeneration biologists. Model systems that have an endogenous capacity for regeneration serve to both probe mechanisms guiding the regenerative response, and to test approaches for inducing or otherwise enhancing a non-regenerating injury. For example, the regenerating urodele limb represents a model for limb regeneration, and the formation of accessory limbs from a lateral wound site serves as a gain of function model for induced regeneration (Endo et al., 2004). In rodents, the regeneration of the digit tip represents an endogenously regenerating system, whereas amputation at a more proximal level serves as a site to identify ways to induce regeneration (Han et al., 2008; Muneoka et al., 2008). Using the neonatal mouse as a model, Yu et al. (2010) demonstrated that digit tip regeneration requires BMP signaling, and that the regeneration of the terminal phalangeal element (P3) could be induced by treating amputation injuries with either BMP2 or BMP7. Since this induced regenerative response is mediated by the formation of a digit blastema, this study represented the first clear demonstration of an induced epimorphic regenerative response of a mammalian limb structure, and as such, establishes a proof of concept that induced regeneration in mammals is possible.

In mammals, BMP signaling is known to play a critical role in the formation of skeletal elements (Bandyopadhyay et al., 2006), is required for skeletal repair following fracture injury (Tsuji et al., 2006), and induces ectopic bone formation in soft tissues such as muscle (Reddi, 1998). BMP7 also induces bone growth when applied to neonatal limb amputations in mice (Ide, 2012; Masaki and Ide, 2007). In amphibian limb regeneration, BMP signaling has not been studied extensively but it likely plays a similar role in skeletogenesis and fracture healing (Satoh et al., 2010), and it appears to be important for joint formation (Satoh et al., 2005). There are a number of known signaling pathways that are linked to the control of limb regeneration (Brockes and Kumar, 2005; Gardiner, 2005; Sanchez Alvarado and Tsonis, 2006), and the evidence suggests that the regenerative response involves a stepwise cascade of the sequential signaling events (Endo et al., 2004). In considering regenerative failure in mammals with respect to such a model, we speculate that defects in one or more signaling pathways could be responsible for a failed regenerative response. In the case of the rodent digit model, the ability of BMP2 or BMP7 to rescue a regenerative response identifies this signaling pathway as the only defect for neonatal regeneration. Whether or not additional signaling pathways are defective in amputations at more proximal levels or in more mature tissues is an important issue that will have to be considered as we move toward a goal of enhancing regenerative capabilities in humans.

The mouse digit tip is a relatively simple regeneration model that involves a single skeletal element and includes the nail organ which is absent at more proximal amputation injuries. To study the role of BMP signaling in a more complex regenerative response we have carried out a series of studies on the regeneration of digits amputated through the second phalangeal element (P2) of neonatal mice. In this model a complete regenerative response would involve regeneration of the distal end of the P2 element, the P2/P3 joint and the P3 element. We find that BMP2 induces the regeneration of the amputated distal end of the P2 element, but we do not observe the formation of joint tissues or the P3 element. Thus, the BMP2-induced regenerative response is restricted to the individual skeletal element that is amputated. We show that BMP2-induced skeletal elongation occurs by the regeneration of an endochondral ossification center at the amputated stump that forms an apical growth zone that directs skeletal elongation. By comparing BMP2-induced regeneration from at two distinct amputation levels, we provide evidence that digit cells utilize positional information to control the polarity of the induced regenerative response. Finally, based on our findings on neonatal digit regeneration, we carried out limb amputation studies on adult mouse

hindlimbs and found that targeted BMP-2 treatment induces patterned skeletal regeneration that involved a distally localized endochondral ossification response. These studies identify the BMP signaling pathway as critical for coordinating the interface between positional information and the stimulation of a segment-specific regenerative response in both neonatal and adult mice.

Materials and Methods

Amputations and BMP2 Treatment

Wild-type CD1 mice used in this study were purchased from Harlan Laboratories (Indianapolis, IN). A BRE-*Gfp* transgenic reporter line (Monteiro et al., 2008) was kindly provided by Dr. Christine Mummery (Hubrecht Institute, Netherlands). For digit studies, postnatal day 3 (PN3) neonates were anesthetized as previously described (Han et al., 2008) and amputation through the middle of the second phalanx (P2) of digits 2 and 4 of both hindlimbs were carried out (Fig. 1A). For BMP2 treatment of digit amputation, we used Affi-Gel Blue Gel beads (Bio-Rad, Hercules, CA) soaked with recombinant human BMP2 (0.5 μg/μl; R&D System, Minneapolis, MN) or BSA (0.1% in PBS) as previously described (Yu et al., 2010). Bead implantation was carried out after wound closure (4 days post-amputation, DPA) and targeted the region between the wound epithelium and the skeletal stump (Fig. 1A). In other studies BMP2 or BSA containing beads were implanted into the proximally amputated terminal phalanx (P3) at 4 DPA as previously described (Yu et al., 2010). As a positive control for BMP activity we used enhanced chondrogenesis of micromass cultures of E14 digit cells. For proliferation studies, BrdU (45 μg/g body weight) or EdU (2.52 μg/g body weight) was injected IP, and tissue was collected 2 hours later.

For limb regeneration studies, adult (8–10 weeks old) CD1 mice were used. Mice were anesthetized and treated with an analgesic (Buprenex 0.17 μg/g body weight, i.p.). One hindlimb was shaved at the level of the shank and the limb was scrubbed with Povidone-Iodine (Dynarex). Amputation was made with sharp scissors through the mid-shank region transecting proximal to the level where the tibia and fibula fused (Fig. 6A). Bleeding was initially controlled using sterile cotton tip applicators then the wound was covered with DermaBond (Ethicon). In all studies wound healing was monitored visually and completion of epidermal closure was verified histologically. For BMP2 treatment, gelatin gel discs (Ide, 2012) (kindly provided by Dr. Hirouki Ide, Tohoku University) containing 1.0 mg/ml of hrBMP-2 (kindly provided from Dr. Senyon Choe, Salk Institute) or BSA (0.1% in PBS) were implanted between the wound epithelium and the limb stump. Experimental and control limbs were monitored by in vivo imaging using μCT at 1, 2, 3, 6, 8 and 10 weeks post-amputation (WPA). For histological analysis and immuno-staining of type II collagen, amputated limb samples were fixed at 17 DPA and 6 WPA. All surgical procedures used in this study were in compliance with the standards for the care and use of animals approved by Tulane University's Institutional Animal Care and Use Committee.

Histological analyses

For whole mount skeletal analysis, digit samples were collected at 14, 21 and 42 DPI and stained with Alizarin red as described by Han et al. (2008). To quantify bone elongation we measured the proximal-distal length of the P2 bone at 14 days post bead implantation (DPI) for experimental and control groups (n = 24–36 digits/group). For histological, immunohistochemical, and in situ hybridization studies, samples were collected at 1, 3, 7 and 11 DPI, and section tissues were prepared as previously described (Han et al., 2008; Yu et al., 2010). To examine the gene expression during the processes of digit regeneration, antisense ribo-probes for *Type II Collagen (Col2a1), Type X Collagen (Col10a1), Osteocalcin (Ocn), Msx1* and *Pedf* were generated by using the Digoxigenin-UTP

transcription labeling Kit (Roche, Indianapolis, IN) according to the manufacturer's instruction. All ribo-probes have been previously described (Han et al., 2008; Yu et al., 2010). Section in situ hybridization was performed as described previously (Han et al., 2003), and in most cases analyses were carried out on adjacent serial sections. Fluorescent in situ hybridization (FISH) was used to detect *Col2a1* and *Col10a1* co-expression on tissue sections. The FISH procedure was similar to our single probe protocol with the following changes. The *Col10a1* probe was synthesized using the Fluorescein RNA labeling mix (Roch) and anti-DIG-POD and anti-Fluorescein-POD were used as secondary antibodies. Tyramide signal amplification kits (invitrogen), Alex Fluor 488, and Alexa Fluor 568 were used to detect signals separately. A quenching step was used after detecting the *Col2a1* signal.

Cell proliferation studies using BrdU incorporation was carried out using the BrdU labeling and detection Kit II (Roche, Indianapolis, IN). Quantification of BrdU incorporation is based on cell counts of 5,000 μm^2 fields from representative sections of 5 digits as previously described (Yu et al., 2010). Student's t-test was used to establish significance and error bars represent standard deviation. Combined cell proliferation and immunohistochemical analysis used the Click-iT EdU Imaging Kit (Invitrogen) following the manufacturer's suggested protocol for immunostaining. For collagen II immunostaining we used the a mouse anti-mouse collagen type II alpha 1 chain monoclonal antibody (Acris Antibodies, San Diego, CA) and Alexa Fluor 488 goat anti-mouse IgG (Invitrogen). For GFP immunostaining we used a chicken anti-GFP polyclonal antibody (Novus Biologicals, Littleton, CO) and Alexa Fluor 647 goat anti-chicken IgG (Invitrogen).

Micro-computed tomography (μCT)

Regenerated P2 digit samples at PN21 and amputated adult hindlimbs at varying time points were scanned using the vivaCT 40 (SCANCO Medical, Wayne, PA) as previously described (Fernando et al., 2011). Bone samples were imaged with high-resolution settings (voxel size 10.5 μm and Energy 55 kVp) and saved as dicom files. The serial section files were processed to construct 3-dimensional images using the BoneJ plugin of Fiji. Length measurements were carried out directly from reconstructed images.

Results

Induced regeneration of P2 bone by BMP2 treatment

Previously we demonstrated that a regenerative response following amputation through the proximal region of the terminal phalanx (P3) can be induced by either BMP7 or BMP2 (Yu et al., 2010). Since the terminal phalangeal bone has inherent regenerative capabilities when amputated at a distal level (Han et al., 2008), one possibility is that a regulatory role for BMP signaling in digit regeneration is restricted to the terminal phalangeal element. Alternatively, BMP signaling may also be critical for regeneration from proximal regions of the neonatal digit. We carried out regeneration induction studies on neonatal digits amputated midway through the P2 element followed by treatment with BMP2 to determine if an enhanced regenerative response is elicited (Fig. 1A). Amputation at the level of the P2 element of the neonatal or adult mouse does not result in an endogenous regenerative response, instead the amputation injury undergoes a wound healing response and the P2 element remains truncated (Agrawal et al., 2010; Gourevitch et al., 2009; Neufeld, 1985; Wang et al., 2010; Yu et al., 2010). For these studies we amputated midway through the P2 element at PN3 and implanted the BMP2 microcarrier bead between the wound epithelium and the skeletal stump at 4 DPA when wound closure is complete (Yu et al., 2010; Fig. 1A). We found that a single application of BMP2 can induce an enhanced digit elongation

response when compared to control amputated digits (Fig. 1B). We noted a dramatic elongation response in digits collected at 28 DPI.

We carried out an initial series of digit amputation and BMP2 induced regeneration studies in which we analyzed the response using whole mount skeletal staining and histology. Control P2 amputations without treatment or receiving a BSA-containing control microcarrier bead fail to display any indication of a regenerative response by 14 DPI (Fig. 1C), whereas P2 amputations treated with a single BMP2-containing microcarrier bead displayed phalangeal elongation (Fig. 1D). Analysis of whole-mount Alizarin red stained samples indicate that the induced regenerative response is restricted to the distal region of the P2 element; we found no evidence for the regeneration of the P2/P3 joint or the P3 element. Thus, despite the fact that BMP2 can induce P3 regeneration from P3 amputations (Yu et al., 2010), it does not induce P3 regeneration from a P2 level amputation. Instead, our finding shows that BMP2 is able to induce the regeneration of the amputated distal region of the P2 element. Quantitative measurements at 14 DPI demonstrate that the BMP2 induced elongation response is statistically significant as compared to BSA treated controls (Fig. 1E), and that the proximal-distal length of the P2 element was restored to 88% of similar staged unamputated controls. Consistent with this conclusion, a surface 3-dimensional μCT analysis of induced P2 regeneration indicates that it is impossible to distinguish the regenerated bone from the stump bone (Fig. 1F), although analysis of radiographic sections clearly shows irregularities associated with the level of amputation (Fig. 1G). The combination of the skeletal anatomy along with the smooth integration with the stump bone suggests that BMP2 induces a segmental regenerative response that replaced the amputated region of the P2 element.

One key observation from these studies is that the positioning of the BMP2 microcarrier bead is consistently at the distal tip of the induced outgrowth, whereas control beads are rarely maintained at a distal location. Since the Affigel blue agarose bead that we use as a carrier is non-adherent to tissues after implantation, the fact that it is maintained at a distal position suggests that it is physically constrained by the elongation of the bone stump. This is particularly striking in samples in which the positioning of the BMP2 bead shifted to a lateral position during the response causing regenerated bone growth to deviate from the digit's proximal-distal axis (Fig. 1H). While this response appears abnormal, the regenerated bone maintains continuity with the stump bone indicating that it is not an example of ectopic bone formation. These observations suggest that the spatial localization of the BMP2 source plays a role in organizing the pattern of the regeneration response.

BMP2 induced regeneration is mediated by the formation of an endochondral ossification center

Neonatal digit amputation at the P2 level undergoes a wound healing response with no evidence of digit elongation. Following P2 amputation, epidermal closure is complete in 4–5 days (Yu et al., 2010) and implantation of a BSA treated control bead at 4 DPA does not influence the wound healing response. By 3 DPI cells contiguous with the dermis invade the wound site and there is evidence of wound contraction that brings mature epidermal structures as well as amputated tendon tissue to the apical periphery of the wound (Fig. 2A). Histological observations indicate that the fibrous tissue build up between the P2 stump and the apical epidermis becomes vascularized between 3 and 7 DPI (Fig. 2B,C). The digit stump at 5 DPI is composed of hypertrophic chondrocytes and by 7 DPI osteoblast differentiation across the apex of the stump is initiated (Fig. 2D). In situ hybridization studies indicate that cells distal to the amputation stump do not express either *Col2a1* or *Col10a1* at any time following treatment with BSA (not shown).

The BMP2-induced regenerative response is associated with an initial accumulation of mesenchymal cells distal to the P2 stump that forms an endochondral ossification center at the distal apex of the amputated stump. An aggregation of mesenchymal cells associated with the BMP2 bead and contiguous with the P2 stump is clearly evident at 3 DPI (Fig. 2E). At this stage there is no clear histological evidence of chondrocyte differentiation however, a large aggregate of chondrogenic cells distal to the stump is identified based on the expression of *Col2a1* (Fig. 2E′). These differentiating chondrocytes are not directly associated with the BMP2 bead, and there are no cells in the regenerating apex expressing the hypertrophic chondrocyte marker *Col10a1* (Fig. 2E″). By 5 DPI overt chondrogenesis contiguous with the P2 element is seen histologically (Fig. 2F), and cells extending from the stump distally express *Col2a1* (Fig. 2F′). There is a distal population of mesenchymal cells associated with the BMP2 bead that separate *Col2a1* expressing chondrocytes from the BMP2 source. *Col10a1* transcripts in the regenerate are first observed at 5 DPI extending distally from the stump indicating the differentiation of hypertrophic chondrocytes (Fig. 2F″). The progression of *Col2a1* expressing chondrocytes to *Col10a1* expressing hypertrophic chondrocytes is indicative of an endochondral ossification response associated with BMP2 induced regeneration. By 7 DPI overt chondrogenesis contiguous with the P2 element and the BMP2 bead is seen histologically (Fig. 2G), and *osteocalcin* expressing cells are first observed at the interface between the P2 stump and the proximal regenerate (Fig. 2H).

During endochondral ossification the Col II expressing chondrocytes differentiate into Col X expressing hypertrophic chondrocytes and this differentiation program plays a critical role in skeletal growth. To address whether a similar program of differentiation occurs during BMP2-induced regeneration, we used two color FISH to identify cells co-expressing *Col2a1* and *Col10a1* as they transition between these two differentiative states. During endochondral ossification in P2 proximal growth plates of at stage matched control digits (PN14), the majority of cells express either *Col2a1* or *Col10a1*, however at the interface between proliferating chondrocytes and hypertrophic chondrocytes transcripts for both marker genes can be found in a few cells (Fig. 2I). In BMP2-induced regenerates at 7 DPI (PN14) we similarly observe the majority of cells either expressing *Col2a1* or *Col10a1*, and we also find cells expressing both chondrocytic marker genes (Fig. 2J). These data provide evidence that during BMP2-induced regeneration, a functionally organized endochondral ossification center is established de novo at the amputated P2 stump in which chondrocytes aggregate and differentiate into hypertrophic chondrocytes. The hypertrophic chondrocytes establish a scaffold for the invasion of osteoblasts associated with the regeneration of new bone tissue.

Pattern Formation and BMP2 induced regeneration

Since BMP2 can induce a regenerative response from two distinct amputation levels (proximal P3 and P2), we wanted to study the role that amputation level plays in patterning the regenerative response. Bone formation during digit development involves endochondral ossification and the differentiation of *Col2a1* expressing chondroctyes into *Col10a1* expressing hypertrophic chondrocytes establishes the polarity of skeletal elongation. Ossification of the P3 element progresses from distal to proximal whereas the P2 element progresses from a central region toward both ends (Han et al., 2008). In a previous study we found that amputation at a proximal (non-regenerating) level of the P3 element was stimulated to regeneration with either BMP2 or BMP7 treatment (Yu et al., 2010). Focusing specifically on BMP7 we found that the regenerative response was associated with the induction of endochondral marker genes whose expression mimicked the development of the P3 element. To determine whether BMP2 induced a similar endochodral ossification response we collected BMP2-induced regenerates from proximal P3 amputations at 7 DPI for in situ hybridization studies. We found that the pattern of endochondral marker gene

expression induced by BMP2 was identical to that of BMP7 and followed the pattern displayed during P3 development; *Col2a1* was expressed proximally and *Col10a1* was expressed distally (Fig. 3A,B). Thus, the polarity of BMP2-induced ossification in proximal P3 regenerates is distal to proximal.

BMP2-induced regeneration of P2 amputation involves the formation of a new distal endochondral ossification center. The developmental ossification of the distal region of the P2 element has a polarity that is opposite to that of the P3 element, i.e. *Col2a1* is expressed distally and *Col10a1* is expressed proximally. To determine whether endochondral ossification during BMP2-induced P2 regeneration follows a developmental pattern we examined the expression pattern of *Col2a1* and *Col10a1* at 7 DPI. At this timepoint the expression of endochondral marker genes is robust and the spatial expression of *Col2a1* is associated with the distal BMP2 bead (Fig. 3C) whereas the expression domain of *Col10a1* is associated with the proximal stump (Fig. 3D). These results show that at P2 amputations BMP2 induces an endochondral ossification center that is similar to the developmental pattern and is of opposite polarity to the BMP2-induced endochondral ossification response observed during proximal P3 induced regeneration.

These studies examining the segment-specific regenerative response elicited by BMP2 following digit amputation show that the patterning of chondrocyte differentiation during induced regeneration is not dictated by the inducer, but instead controlled by cells at the amputation wound (Fig. 3E). We conclude that during induced digit regeneration in mammals, cells at the respective wound sites react to BMP2 in a position-specific manner, i.e. they display positional information. These data provide evidence that mammalian tissues that lack regenerative ability still possess and/or are able to re-acquire positional information that is necessary to participate in a functional regenerative response that is appropriate for the amputation level.

Blastema formation and BMP2 induced P2 regeneration

The regeneration of a mammalian digit, whether endogenous or induced, is associated with the formation of a blastema of proliferating cells (Han et al., 2008; Yu et al., 2010). To characterize the BMP2-induced P2 regenerative response, we first analyzed cell proliferation based on BrdU incorporation. Control amputations treated with a BSA microcarrier bead displayed a low level of BrdU incorporation throughout the connective tissue and bone stump at 3 DPI (Fig. 4A) and 7 DPI (Fig. 4C) indicating that an enhanced proliferative response does not occur in amputated digits that fail to regenerate. Alternatively, amputated digits treated with BMP2 displayed a robust proliferation response that was initially localized to connective tissue cells distal to the bone stump and associated with the microcarrier bead at 3 DPI (Fig. 4B). At 7 DPI proliferating cells are detected in distal tissue associated with the BMP2 bead, and also associated with the regenerating stump (Fig. 4D). Quantitative analyses at 3 and 7 DPI confirm that the proliferative response to BMP2 treatment can be divided into two distinct phases; an initial proliferative burst within the connective tissue associated with the BMP2 bead at the amputation wound and a secondary burst of proliferation in the regenerating P2 stump (Fig. 4E). This proliferative response is transient since few BrdU labeled cells are detected by 11 DPI (not shown).

To investigate the link between BMP2 signaling and growth stimulation during induced regeneration, we utilized a BRE-*Gfp* transgenic reporter mouse line in which the pSMAD responsive *Id1* promoter is used to drive *Gfp* expression (Monteiro et al., 2008). To study growth stimulation we combined immunohistochemical analyses for GFP with EdU incorporation (Salic and Mitchison, 2008). At 3 DPI when there is a significant increase in proliferation of mesenchymal cells in BMP2-treated amputations as compared to BSA controls, we find a number of EdU positive cells that co-express GFP (Fig. 4F). This

indicates that canonical BMP signaling is associated with proliferating cells within the BMP2-induced endochondral ossification center. In BSA-treated control samples we observe few GFP positive cells, few EdU positive cells, and no double labeled cells (not shown). To explore whether BMP signaling is associated with the initiation of proliferation in BMP2-induced regeneration, we carried out double labeling studies at 1 DPI using the BRE-*Gfp* reporter mouse and EdU incorporation. At this early timepoint we found that many double labeled mesenchymal cells localized to the region between the BMP2 bead and the P2 stump (Fig. 4G). These findings are consistent with the conclusion that BMP2 signaling stimulates cell proliferation via a pSMAD mediated pathway, and suggest that this early proliferation response initiates the formation of the endochondral ossification center induced by BMP2 during the regenerative response.

The proliferative response along with the initiation of proximal differentiation of the 3 DPI mesenchymal aggregate induced by BMP2 is suggestive of a regenerative response involving blastema formation. Blastema formation occurs during endogenous digit tip regeneration (Fernando et al., 2011; Han et al., 2008; Muneoka et al., 2008) and blastema marker genes are expressed during BMP7 induced regeneration of proximal P3 amputations (Yu et al., 2010). To explore blastema formation in BMP2 induced P2 amputations we examined the expression of two blastema marker genes, *Msx1* and *Pedf*, within the distal region of the induced regenerate at 3 DPI. In both control non-regenerating amputations and BMP2-induced regenerates at this stage we failed to find cells expressing either of the two blastema marker genes (not shown). However, at 1 DPI we found that both blastemal markers were expressed in the distal mesenchyme. *Msx1* transcripts were expressed primarily by cells closely associated with the BMP2 bead (Fig. 4H), whereas *Pedf* expressing cells were scattered throughout the BMP2 treated amputation wound and not restricted to the region surrounding the BMP2 bead (Fig. 4J). Control samples treated with a BSA bead failed to induce either *Msx1* or *Pedf* expression at the amputation wound (Figs. 4I,K). These findings suggest that a blastema phase of the BMP2-induced P2 regenerative is present but transient.

Regeneration of a modified growth plate

In our studies on BMP2 induced P2 regeneration we found both histological and molecular evidence that both proliferating cells and differentiated chondrocytes are present at 3 DPI. To determine whether BMP2 induced regeneration involved the proliferation of chondrocytes, we used EdU labeling and Col II immunohistochemistry to identify proliferating chondrocytes. In BSA control studies at 3 DPI we found no cells in the amputation wound site that were double labeled with EdU and Col II (Fig. 5A). On the other hand, in BMP2 treated amputations at 3 DPI, we observed EdU labeled cells localized between the stump and the BMP2 bead, some of which were surrounded by Col II positive extracellular matrix (Fig. 5B,C). These double labeled cells are suggestive of a population of proliferating chondrocytes. To address whether chondrocyte proliferation is maintained during endochondral outgrowth, we analyzed 7 DPI regenerates, a stage where all phases of P2 stump elongation by endochondral ossification are observed (see Figure 2). At this stage EdU incorporation is restricted to the distal region of the regenerate and many of the proliferating cells are also positive for Col II (Fig. 5D,E). Since the EdU marker is nuclear and the Col II immunohistochemistry identifies an extracellular component, it raised the possibility that the proliferating cells may not be the same cells that produced the surrounding matrix. To address this possibility we combined EdU labeling with fluorescent in situ hybridization for *Col2a1* to determine if cells with nuclear EdU labeling also contained cytoplasmic *Col2a1* transcripts during induced endochondral ossification. Using this approach we confirmed the presence of proliferating chondrocytes within the BMP2-

induced mesenchymal cell aggregate at 3 DPI (Fig. 5F), and the apical proliferation zone at 7 DPI (Fig. 5G).

These data are consistent with the general conclusion that BMP2 induces a functional endochondral ossification center in which the apical proliferation and proximal differentiation of chondrocytes is organized in a way so as to direct a patterned skeletal regenerative response. The presence of an apical zone of proliferating chondrocytes induced by BMP2 that differentiate into hypertrophic chondrocytes proximally is reminiscent of growth plate formation during skeletal elongation. While this proliferation zone is not histologically organized into a traditional growth plate with chondrocytic columns of proliferating cells, we note that many chondroctyes have a flattened morphology (see Fig. 5D,E) and display with a distinctively bi-polar intracellular localization of *Col2a1* transcripts (see Fig. 5F,G) as observed in a forming growth plate (see Fig. 2I). Based on these observations it appears that the apical proliferation response during induced regeneration involves the transient formation of a structure simulating a growth plate that drives skeletal elongation associated with the regenerative response.

Skeletal regeneration from limb amputations

Our studies on the neonatal digit model show that targeted application of BMP2 can successfully enhance skeletal regeneration following amputation and the process involves creating a new endochondral ossification center with an apical zone of proliferating chondrocytes. A similar anatomical response has been demonstrated following application of BMP7 to neonatal limb amputations, although skeletal growth is ectopic and discontinuous with the stump (Masaki and Ide, 2007). Using findings from our induced digit regeneration model as a guide we carried out a series of experiments treating adult hindllimb amputations with BMP2 (Figure 6A). Simple amputation through the tibia and fibula displayed a wound healing response in which mature skin contracted over the amputation wound resulting in an irregularly shaped wound epithelium by 2 WPA (Fig. 6B). Histological analyses identified a distinct wound epithelium in regions between the contracted mature skin tissues (Figure 6C) and underlain by connective tissue covering the amputated skeletal stump.

To test the effect of targeted BMP2 treatment on skeletal elongation, amputated limbs were allowed to undergo wound closure prior to the implantation of a gelatin carrier soaked in either BMP2 or BSA at 2 WPA. These limbs were followed using μCT throughout the experiments so we were able to obtain anatomical data at multiple time points for each individual limb studied. μCT analyses of BSA treated control amputations at 1, 3, and 8 weeks post-amputation identified a small amount of bone elongation (Fig. 6D) that appears similar to a previous report of partial regeneration following limb amputation in juvenile rats (Becker, 1972). In some cases irregular hypertrophic bone growth response was observed from simple amputation (not shown), thus the amputation wound displays an inherent capacity to generate new bone tissue during the healing response. Overall, limb amputations with or without BSA treatment resulted in an ossification response that added an average of 1.31 mm (SD = 0.33 mm) of new bone distal to the level of amputation. On the other hand amputated limbs treated with BMP2 displayed directed skeletal elongation and a regenerative response of both the tibia and fibula (Fig. 6E). In the BMP2 group, one sample (n = 1/3; 33%) showed skeletal elongation and complete fusion of the tibia and fibula distal to the amputation, whereas the other two samples showed distal elongation of the tibia and fibula without distal fusion. The distal fusion of the tibia and fibula is suggestive of an appropriate patterning response associated with BMP2-induced regeneration. The mean skeletal elongation response stimulated by BMP2 was over twice the control response (3.04 mm; SD = 0.07 mm) and was significantly greater than control amputations based on a two-tailed student t-test ($P<0.001$). Histological studies of both control and BMP2 treated limbs

at the termination of the study (8–10 weeks) showed only bone tissue at the amputation site and no evidence of cartilage (not shown). BMP2-induced regenerates collected at 4 weeks post-treatment and analyzed for evidence of endochondral ossification based on histological staining and immunohistochemical staining for Col II expression showed apically localized regions of endochondral ossification capping the elongating skeletal elements (Fig. 6F,G). These findings are consistent with the conclusion that skeletal elongation was caused by directed endochondral ossification similar to the mechanism identified in BMP2-induced P2 regeneration.

Discussion

Mammals, including humans, possess limited regenerative capacities whereas other tetrapod vertebrate groups such as urodele amphibians can perfectly replace complex structures including the tail, jaw, and limb (Brockes and Kumar, 2005; Gardiner, 2005; Sanchez Alvarado and Tsonis, 2006). Using the endogenous regenerative response of the mouse digit tip as a model system, we have identified the BMP signaling pathway as required for a regenerative response (Han et al., 2003) and have shown that non-regenerating amputation injury within the terminal phalangeal element can be induced to regenerate with BMP treatment (Yu et al., 2010). In the current study we explore induced regeneration from a more proximal amputation level to determine whether BMP2 treatment can induce regeneration of complex structures (i.e. multiple skeletal structures). We find that BMP2 treatment does not induce a complete regenerative response, but does induce the regeneration of amputated skeletal elements. Our data provide evidence that BMP plays a key role in stimulating regeneration within a skeletal segment but is by itself insufficient to stimulate the regeneration of more distal segments despite the fact that those individual skeletal segments can be induced to regenerate by BMP2. Importantly, we provide evidence that BMP2 treatment is effective in inducing a patterned regenerative response in adults following limb amputation. On the one hand, the demonstration that regeneration of an amputated skeletal stump in neonates and adults is possible represents a novel and important discovery, but the absence of a more complete regenerative response indicates that there remains much to be learned to solve the regeneration problem in mammals. Our data demonstrate the feasibility of induced mammalian regeneration, and suggest that BMP signaling represents a key requirement for induced limb regeneration.

BMP2 induces the regeneration of an endochondral ossification center

The neonatal P2 element at the time of amputation is undergoing endochondral ossification at both distal and proximal ends of the skeletal element, and amputation removes the distal component. Treatment with a point source of BMP2 initiates the regeneration of a new endochondral ossification center at the amputated bone stump that appears similar to the distal ossification center that was amputated. The process begins soon after BMP2 treatment with enhanced proliferation by BMP responsive cells at the amputation wound. During this early phase we also observe the transient expression of blastemal marker genes, *Msx1* and *Pedf. Msx1* is involved in the inhibition of cell differentiation during development (Hu et al., 2001), induces dedifferentiation in myogenic cells (Odelberg et al., 2000) and is functionally required for embryonic digit tip regeneration (Han et al., 2003), thus it seems likely that inhibiting the differentiative state of cells at the injury site is critical for initiating a regenerative response. *Pedf* is expressed in the forming digit marrow (Muneoka et al., 2008) and is known to have anti-angiogenic activity (Filleur et al., 2009). The digit tip blastema in mice is characterized by reduced vascularity (Fernando et al., 2011) and the expression of *Pedf* during induced regeneration suggests that inhibiting vascularization following wound closure is a second critical requirement for a regenerative response. In combination, our

results indicate that BMP2 has multiple effects on the amputation wound including stimulating cell proliferation, inhibiting differentiation and inhibiting angiogenesis.

The next phase in BMP2-induced regeneration is the accumulation of mesenchymal cells that form a de novo endochondral ossification center just distal to the amputated skeletal stump. The endochondral ossification center contains proliferating chondrocytes that form an elongating chondrogenic rod directed toward the BMP2 bead. Elongation appears to be driven by an apical zone of proliferating chondrocytes that display some characteristics of a growth plate and differentiate into hypertrophic chondroctyes in a proximal to distal manner. The final phase of the response involves the invasion of osteoblasts that progresses in a proximal to distal sequence and culminates with the formation of newly regenerated bone that is integrated with the amputated stump. The BMP2-induced regenerative response differs from the initial formation of the distal P2 element which does not form a growth plate during development (Ogden et al., 1994; Reno et al., 2006). The presence of proliferating chondrocytes during the early stages of the induced regenerative response could be related to the unique ability of chondrocytes to dedifferentiation (see Schulze-Tanzil, 2009), and/or to transdifferentiate as has been documented during amphibian limb regeneration (Dunis and Namenwirth, 1977; Kragl et al., 2009; Lheureux, 1983; Namenwirth, 1974). Recent studies suggests that transdifferentiation does not occur during an endogenous digit tip regenerative response in mice (Lehoczky et al., 2011; Rinkevich et al., 2011), although not all cell lineages were not investigated and chondroctyes are not involved in digit tip regeneration (Fernando et al., 2011; Han et al., 2008). The stimulation of an apical zone of proliferating chondrocytes represents a foundation for exploring segment-specific *de novo* skeletal regeneration by effectively regenerating a growth plate.

Regeneration and positional information

One of the hallmarks of regenerative responses centers on the fact that regardless of the extent of injury the regenerative response results in a structurally complete replacement of only those parts of the pattern that is lost. Because of this, virtually all regeneration models invoke the idea that cells involved in the amputation injury response must possess or obtain information about their position within the structure (positional information) that can be used to determine the extent of the injury and to modulate the subsequent response that accurately restores the missing parts of the pattern (French et al., 1976; Wolpert, 1969, 2011). Early studies on the regenerating amphibian limb identified tissues that possess positional information, and fibroblastic cells of the connective tissue as a critical cell type (Bryant, 1987). While the molecular basis of positional information remains unsolved, retinoic acid has been shown to be an important effector of positional information (Bryant and Gardiner, 1992; Maden, 1982) that influences specific cell signaling pathways (da Silva et al., 2002), cell adhesion (Crawford and Stocum, 1988), and spatially restricted transcriptional regulators during limb regeneration (Mercader et al., 2005).

In the current age of regenerative medicine, the question of why mammals (i.e. humans) have limited regenerative capabilities is relevant for considering various therapeutic approaches. In particular, it is unclear whether the limited regenerative capabilities displayed by mammals are the result of a defect in the positional network of information that allows spatially correct responses to injury. Consistent with studies on amphibian limb regeneration (Bryant, et al. 1987), microarray analyses in humans indicate that connective tissue fibroblasts are the only cell type that displays spatially distinct transcriptomes (Chang et al., 2002; Rinn et al., 2006), however there is limited experimental evidence of position-dependent regenerative responses in mammals. In this light our finding that BMP2 induces distinct and appropriate regenerative responses from three different normally non-regenerating amputation injuries of the neonatal and adult mouse provides the first clear evidence that mammalian tissues possess positional properties that are spatially activated in

a regenerative response. In our studies on neonatal digit amputations, the position-specific response is reflected in controlling the polarity of chondrocyte differentiation during endochondral ossification of an induced skeletal structure; in a manner similar to digit development, differentiation occurs distal to proximal during P3 regeneration (Yu et al., 2010) and proximal to distal in P2 regeneration. This finding demonstrates that BMP2 is not acting to pattern the regenerative response, but rather appears to activate a level-specific regenerative potential. The demonstration that a positional information network in mammals exists and can be displayed represents a major step in advancing the general idea that mammalian limb regeneration can be successfully induced. In addition, the data suggest that the BMP signaling pathway represents a key component of the interface between regeneration stimulating factors in the wound environment and the positional information network necessary to pattern the response.

Acknowledgments

We thank the Muneoka lab for discussions. Research funded by R01HD043277 and P01HD022610 from the NIH, W911NF-06-1-0161 from DARPA, W911NF-09-1-0305 from the US Army Research Center, and the John L. and Mary Wright Ebaugh endowment fund at Tulane University.

References

Agrawal V, Johnson SA, Reing J, Zhang L, Tottey S, Wang G, Hirschi KK, Braunhut S, Gudas LJ, Badylak SF. Epimorphic regeneration approach to tissue replacement in adult mammals. Proc Natl Acad Sci U S A. 2010; 107:3351–3355. [PubMed: 19966310]

Bandyopadhyay A, Tsuji K, Cox K, Harfe BD, Rosen V, Tabin CJ. Genetic analysis of the roles of BMP2, BMP4, and BMP7 in limb patterning and skeletogenesis. PLoS Genet. 2006; 2:e216. [PubMed: 17194222]

Becker RO. Stimulation of partial limb regeneration in rats. Nature. 1972; 235:109–111. [PubMed: 4550399]

Brockes JP, Kumar A. Appendage regeneration in adult vertebrates and implications for regenerative medicine. Science. 2005; 310:1919–1923. [PubMed: 16373567]

Bryant SV, Gardiner DM. Retinoic acid, local cell-cell interactions, and pattern formation in vertebrate limbs. Dev Biol. 1992; 152:1–25. [PubMed: 1628749]

Bryant SV, Gardiner DM, Muneoka K. Limb development and regeneration. Amer Zool. 1987; 27:675–696.

Chang HY, Chi JT, Dudoit S, Bondre C, van de Rijn M, Botstein D, Brown PO. Diversity, topographic differentiation, and positional memory in human fibroblasts. Proc Natl Acad Sci U S A. 2002; 99:12877–12882. [PubMed: 12297622]

Crawford K, Stocum DL. Retinoic acid coordinately proximalizes regenerate pattern and blastema differential affinity in axolotl limbs. Development. 1988; 102:687–698. [PubMed: 3168786]

da Silva SM, Gates PB, Brockes JP. The newt ortholog of CD59 is implicated in proximodistal identity during amphibian limb regeneration. Dev Cell. 2002; 3:547–555. [PubMed: 12408806]

Dunis DA, Namenwirth M. The role of grafted skin in the regeneration of x-irradiated axolotl limbs. Dev Biol. 1977; 56:97–109. [PubMed: 320068]

Endo T, Bryant SV, Gardiner DM. A stepwise model system for limb regeneration. Dev Biol. 2004; 270:135–145. [PubMed: 15136146]

Fernando WA, Leininger E, Simkin J, Li N, Malcom CA, Sathyamoorthi S, Han M, Muneoka K. Wound healing and blastema formation in regenerating digit tips of adult mice. Dev Biol. 2011; 350:301–310. [PubMed: 21145316]

Filleur S, Nelius T, de Riese W, Kennedy RC. Characterization of PEDF: a multi-functional serpin family protein. J Cell Biochem. 2009; 106:769–775. [PubMed: 19180572]

French V, Bryant PJ, Bryant SV. Pattern regulation in epimorphic fields. Science. 1976; 193:969–981. [PubMed: 948762]

Gardiner DM. Ontogenetic decline of regenerative ability and the stimulation of human regeneration. Rejuvenation Res. 2005; 8:141–153. [PubMed: 16144469]

Gourevitch DL, Clark L, Bedelbaeva K, Leferovich J, Heber-Katz E. Dynamic changes after murine digit amputation: the MRL mouse digit shows waves of tissue remodeling, growth, and apoptosis. Wound Repair Regen. 2009; 17:447–455. [PubMed: 19660054]

Han M, Yang X, Farrington JE, Muneoka K. Digit regeneration is regulated by Msx1 and BMP4 in fetal mice. Development. 2003; 130:5123–5132. [PubMed: 12944425]

Han M, Yang X, Lee J, Allan CH, Muneoka K. Development and regeneration of the neonatal digit tip in mice. Dev Biol. 2008; 315:125–135. [PubMed: 18234177]

Hu G, Lee H, Price SM, Shen MM, Abate-Shen C. Msx homeobox genes inhibit differentiation through upregulation of cyclin D1. Development. 2001; 128:2373–2384. [PubMed: 11493556]

Ide H. Bone pattern formation in mouse limbs after amputation at the forearm level. Dev Dyn. 2012; 241(3):435–41. [PubMed: 22275066]

Kragl M, Knapp D, Nacu E, Khattak S, Maden M, Epperlein HH, Tanaka EM. Cells keep a memory of their tissue origin during axolotl limb regeneration. Nature. 2009; 460:60–65. [PubMed: 19571878]

Lehoczky JA, Robert B, Tabin CJ. Mouse digit tip regeneration is mediated by fate-restricted progenitor cells. Proceedings of the National Academy of Sciences of the United States of America. 2011; 108:20609–20614. [PubMed: 22143790]

Lheureux E. The origin of tissues in the X-irradiated regenerating limb of the newt Pleurodeles waltlii. Prog Clin Biol Res. 1983; 110(Pt A):455–465. [PubMed: 6338527]

Maden M. Vitamin A and pattern formation in the regenerating limb. Nature. 1982; 295:672–675. [PubMed: 7057925]

Masaki H, Ide H. Regeneration potency of mouse limbs. Dev Growth Differ. 2007; 49:89–98. [PubMed: 17335430]

Mercader N, Tanaka EM, Torres M. Proximodistal identity during vertebrate limb regeneration is regulated by Meis homeodomain proteins. Development. 2005; 132:4131–4142. [PubMed: 16107473]

Monteiro RM, de Sousa Lopes SM, Bialecka M, de Boer S, Zwijsen A, Mummery CL. Real time monitoring of BMP Smads transcriptional activity during mouse development. Genesis. 2008; 46:335–346. [PubMed: 18615729]

Muneoka K, Allan CH, Yang X, Lee J, Han M. Mammalian regeneration and regenerative medicine. Birth Defects Res C Embryo Today. 2008; 84:265–280. [PubMed: 19067422]

Namenwirth M. The inheritance of cell differentiation during limb regeneration in the axolotl. Dev Biol. 1974; 41:42–56. [PubMed: 4140121]

Neufeld DA. Bone healing after amputation of mouse digits and newt limbs: implications for induced regeneration in mammals. Anat Rec. 1985; 211:156–165. [PubMed: 3977084]

Odelberg SJ, Kollhoff A, Keating MT. Dedifferentiation of mammalian myotubes induced by msx1. Cell. 2000; 103:1099–1109. [PubMed: 11163185]

Ogden JA, Ganey TM, Light TR, Belsole RJ, Greene TL. Ossification and pseudoepiphysis formation in the “nonepiphyseal” end of bones of the hands and feet. Skeletal Radiol. 1994; 23:3–13. [PubMed: 8160033]

Reddi AH. Role of morphogenetic proteins in skeletal tissue engineering and regeneration. Nat Biotechnol. 1998; 16:247–252. [PubMed: 9528003]

Reno PL, McBurney DL, Lovejoy CO, Horton WE Jr. Ossification of the mouse metatarsal: differentiation and proliferation in the presence/absence of a defined growth plate. Anat Rec A Discov Mol Cell Evol Biol. 2006; 288:104–118. [PubMed: 16342215]

Rinkevich Y, Lindau P, Ueno H, Longaker MT, Weissman IL. Germ-layer and lineage-restricted stem/progenitors regenerate the mouse digit tip. Nature. 2011; 476:409–413. [PubMed: 21866153]

Rinn JL, Bondre C, Gladstone HB, Brown PO, Chang HY. Anatomic demarcation by positional variation in fibroblast gene expression programs. PLoS Genet. 2006; 2:e119. [PubMed: 16895450]

Salic A, Mitchison TJ. A chemical method for fast and sensitive detection of DNA synthesis in vivo. Proceedings of the National Academy of Sciences of the United States of America. 2008; 105:2415–2420. [PubMed: 18272492]

Sanchez Alvarado A, Tsonis PA. Bridging the regeneration gap: genetic insights from diverse animal models. Nat Rev Genet. 2006; 7:873–884. [PubMed: 17047686]

Satoh A, Cummings GM, Bryant SV, Gardiner DM. Regulation of proximal-distal intercalation during limb regeneration in the axolotl (Ambystoma mexicanum). Dev Growth Differ. 2010; 52:785–798. [PubMed: 21158757]

Satoh A, Suzuki M, Amano T, Tamura K, Ide H. Joint development in Xenopus laevis and induction of segmentations in regenerating froglet limb (spike). Dev Dyn. 2005; 233:1444–1453. [PubMed: 15977182]

Schulze-Tanzil G. Activation and dedifferentiation of chondrocytes: implications in cartilage injury and repair. Ann Anat. 2009; 191:325–338. [PubMed: 19541465]

Tsuji K, Bandyopadhyay A, Harfe BD, Cox K, Kakar S, Gerstenfeld L, Einhorn T, Tabin CJ, Rosen V. BMP2 activity, although dispensable for bone formation, is required for the initiation of fracture healing. Nat Genet. 2006; 38:1424–1429. [PubMed: 17099713]

Wang G, Badylak SF, Heber-Katz E, Braunhut SJ, Gudas LJ. The effects of DNA methyltransferase inhibitors and histone deacetylase inhibitors on digit regeneration in mice. Regen Med. 2010; 5:201–220. [PubMed: 20210581]

Wolpert L. Positional information and the spatial pattern of cellular differentiation. J Theor Biol. 1969; 25:1–47. [PubMed: 4390734]

Wolpert L. Positional information and patterning revisited. J Theor Biol. 2011; 269:359–365. [PubMed: 21044633]

Yu L, Han M, Yan M, Lee EC, Lee J, Muneoka K. BMP signaling induces digit regeneration in neonatal mice. Development. 2010; 137:551–559. [PubMed: 20110320]

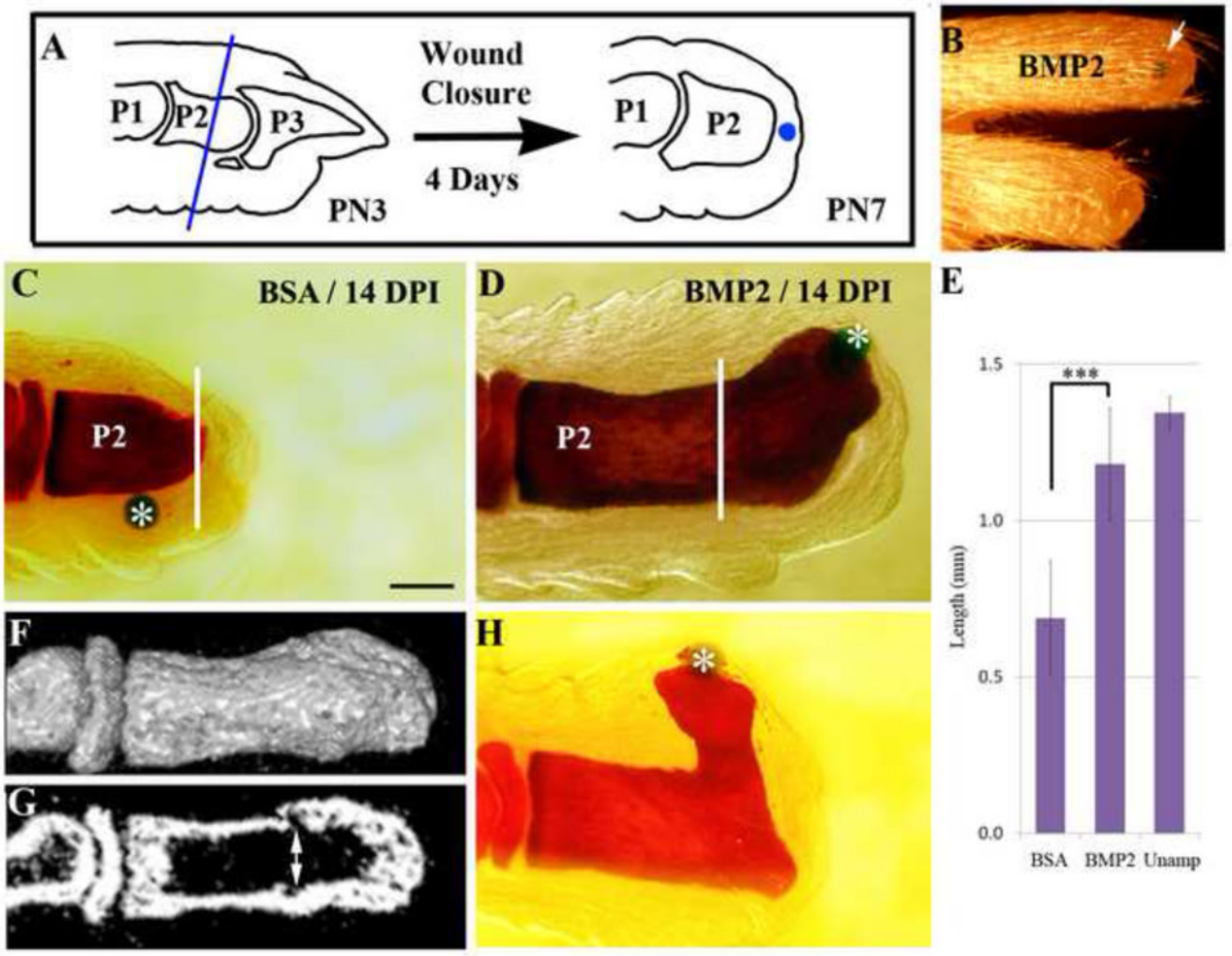

Figure 1. Induced regeneration of the second phalanx (P2)

Distal is toward the right in all images. **A**) Schematic diagram showing amputation level and the positioning of implanted bead following wound closure. PN3 digits are amputated through the middle of the P2 element (blue line). Four days after amputation (PN7), an Affigel blue bead (blue) is implanted into the mesenchymal tissue between wound epithelium and bone stump. **B)** Gross morphology of an regenerated digit (upper) with the BMP2 bead (arrow), and a similarly amputated control digit (lower) at 28 days post-implantation (DPI). **C)** Whole mount bone staining of a control amputated P2 digit (white line) treated with a BSA bead (*) at 14 DPI. **D)** Whole mount bone staining of a BMP2-treated amputated digit at 14 DPI showing skeletal outgrowth from the amputated stump (white line) induced by the BMP2 bead (*). **E)** Statistical comparison of the proximal-distal length of the P2 phalangeal bone at 14 DPI in BSA-treated and BMP2-treated digits in comparison to control unamputated digits (t-test, ± s.e.m., ***, $P < 0.001$). **F)** μCT reconstruction of a BMP2 induced regenerate at 14 DPI showing the smooth integration of the bone surface between the stump and regenerated skeletal tissues. **G)** Radiographic section of the digit displayed in **F** showing internal skeletal tissue irregularities (double arrow) identifying the amputation level and distinguishing the stump from the regenerated bone. Note that the marrow cavity is contiguous between the stump and regenerate. **H**) Whole mount bone staining (14 DPI) of a BMP2-induced regenerate showing bead (*) displacement associated with mis-directed skeletal outgrowth.

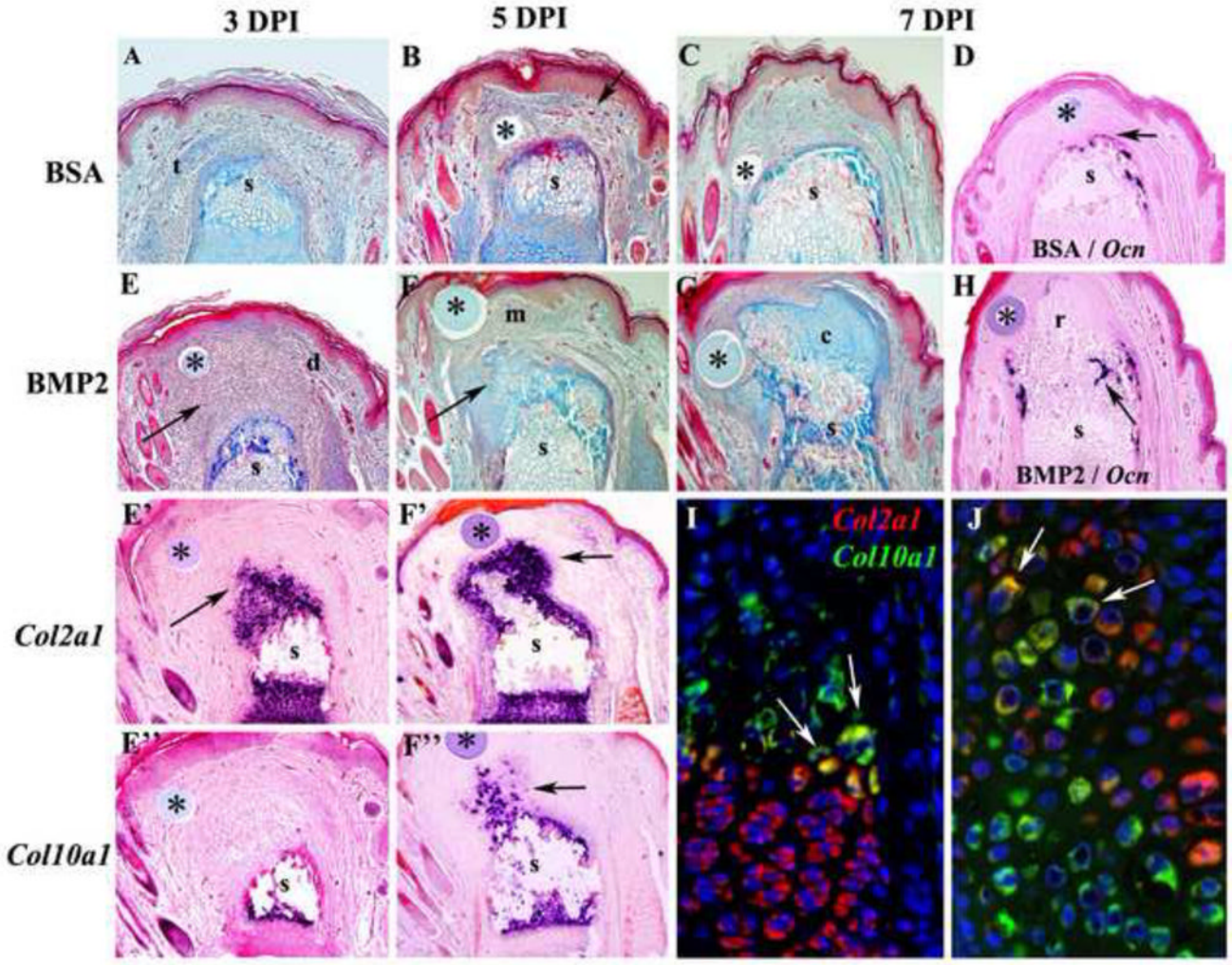

Figure 2. Endochondral ossification during BMP2 induced regeneration

Distal is toward the top in all images and microcarrrier beads are indicated by *. **A–C)** Histological analysis of control BSA-treated P2 amputations. **A)** At 3 DPI there is evidence of wound contraction based on differentiated epidermal structures along the periphery of the stump (s) and encroachment of a severed tendon (t) over the amputated skeletal stump. **B)** At 5 DPI the control amputation wound associated with a BSA bead is composed of vascularized (arrow) fibrous connective tissue covering the skeletal stump (s). **C)** At 7 DPI the amputation wound associated with the control BSA bead continues to accumulate fibrous connective tissue that covers the skeletal stump (s). **D)** Section in situ hybridization at 7 DPI showing cells expressing the osteoblast marker *Osteocalcin* forming a cap over the amputated skeletal stump (s). **E–G)** BMP2-treated P2 amputations. **E)** Histological section at 3 DPI showing the accumulation of mesenchymal cells (arrow) distal to the amputated skeletal stump (s) and associated with the BMP2 bead. The mesenchymal cell mass is flanked with connective tissue of the dermis (d) and is oriented in the direction of the BMP2 bead. **E′)** Section in situ hybridization at 3 DPI showing *Col2a1* transcripts (arrowhead) associated with cells just distal to the skeletal stump (s) and not associated with the BMP2 bead. **E″)** Section in situ hybridization for *Col10a1* transcripts showing the absence of hypertrophic chondrocytes distal to the amputated stump (s) at 3 DPI. **F)** Histological section at 5 DPI showing a reduced population of mesenchymal cells (m) associated with the

BMP2 bead, and chondrocytic tissues (arrow) contiguous with, and distal to, the amputated skeletal stump (s). **F′)** Section in situ hybridization for *Col2a1* transcripts (arrow) showing that chondrocytes associated with the skeletal stump (s) extend distally toward the BMP2 bead. **F″)** Section in situ hybridization for *Col10a1* transcripts (arrow) showing that hypertrophic chondrocytes distal to the amputated stump (s) are present at 5 DPI. **G)** Histological section at 7 DPI showing few distal mesenchymal cells, and a large mass of chondrocytic tissue (c) contiguous with, and distal to, the amputated skeletal stump (s) that is associated with the BMP2 bead. **H)** Section in situ hybridization showing the initiation of *Osteocalcin* expression at the interface between the regenerating tissue (r) induced by the BMP2 bead and the amputated skeletal stump (s) at 7 DPI. **I–J)** Double color fluorescent section in situ hybridization to co-localize *Col2a1* and *Col10a1* transcripts in the proximal P2 growth plate at PN14 (**I**) and a BMP2-induced P2 regenerate at 7 DPI (**J**). **I)** Most growth plate chondrocytes either express *Col2a1* (red) or *Col10a1* (green) transcripts. However, some cells at the interface between proliferating chondrocytes and hypertrophic chondrocytes express both *Col2a1* and *Col10a1* transcripts (arrows), indicating a transitional state during the differentiation process. **J)** In BMP2-induced regenerates most cells either express *Col2a1* (red) or *Col10a1* (green) transcripts, but some co-expressing cells (arrows) are observed at the interface between *Col2a1* expressing and *Col10a1* expressing cells.

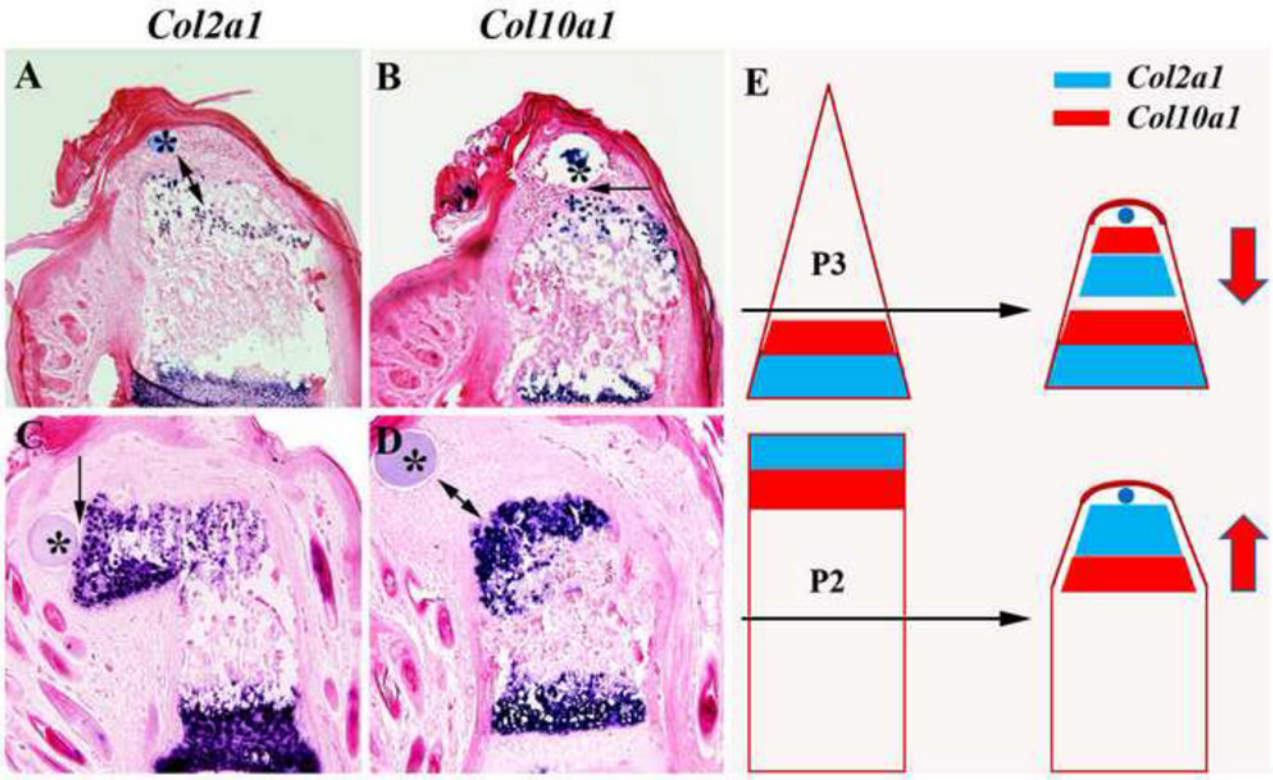

Figure 3. Patterning of BMP2-induced regeneration is level-dependent

Distal to toward the top in all images and microcarrrier beads are indicated by *. **A)** Section in situ hybridization at 7 DPI of a BMP2-induced regenerate from a proximal P3 amputation showing the localization of *Col2a1* expressing chondrocytes relative to the BMP2 bead. *Col2a1* expressing chondrocytes are not in direct contact with the BMP2 bead (double arrow) but are proximally localized. **B)** Section in situ hybridization at 7 DPI of the same BMP2-induced regenerate from a proximal P3 amputation shown in **A**, indicating that the *Co10a1* expressing chondrocytes are in direct contact (arrow) with the BMP2 bead. Relative to the BMP2 bead, the *Col2a1* expressing cells are proximal to the *Col10a1* expressing cells. **C)** Section in situ hybridization at 7 DPI of a BMP2-induced P2 regenerate showing the localization of *Col2a1* expressing chondrocytes relative the BMP2 bead. *Col2a1* expressing chondrocytes are distally localized and in direct contact with the BMP2 bead (arrow). **D)** Section in situ hybridization at 7 DPI of the same BMP2-induced P2 regenerate shown in **C**, indicating that the *Co10a1* expressing chondrocytes are proximally localized and not in direct contact (double arrows) with the BMP2 bead. Relative to the BMP2 bead, the *Col2a1* expressing cells are distal to the *Col10a1* expressing cells. **E)** Diagrammatic summary displaying the shift in polarity of the endochondral ossification centers induced by BMP2 (blue bead) from two different amputation levels (black arrows). The polarity of the endochondral ossification center is depicted by the proximal-distal positioning of the expression domains of *Col2a1* (blue) and *Col10a1* (red). In BMP2-induced regeneration of the proximal P3 amputation the *Col2a1* expression domain is proximal to the *Col10a1*domain, whereas this orientation is reversed for BMP2-induced P2 regeneration. The polarity of the BMP2-induced endochondral ossification is shown by the red arrows. While BMP2 is capable of inducing regenerative responses from two distinct levels, the patterning of the induced regenerative response is level-specific and dictated by the amputation wound rather than by the inducer.

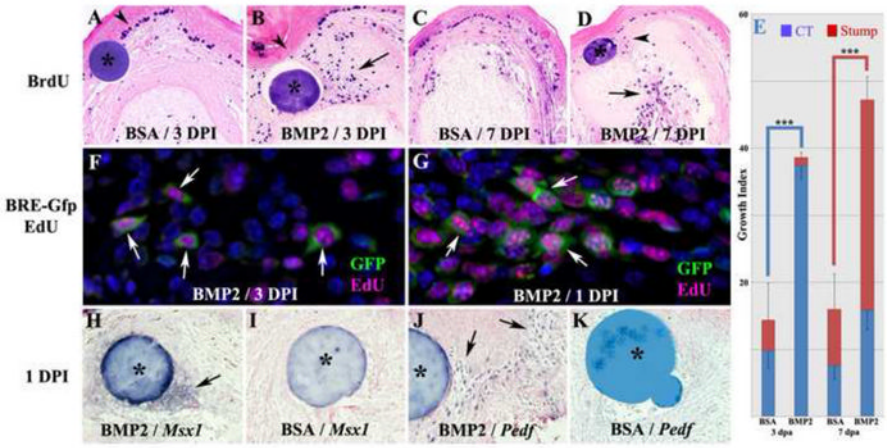

Figure 4. Blastema formation during induced regeneration

Distal is toward the top in all images and microcarrrier beads are indicated by *. **A–E**: BrdU incorporation in BMP2 treated and BSA control amputated digits. **A)** BSA treated amputations at 3 DPI display few BrdU labeled cells that are scattered within the healing dermis and skeletal stump, whereas the basal layer of the wound epithelium displays heavy BrdU labeling (arrowhead). **B.** BMP2 treated amputations at 3 DPI display numerous BrdU labeled cells within the distal mesenchyme (arrow) associated with the healing dermis with few labeled cells in the skeletal stump. There are also few BrdU labeled cells in the wound epithelium associated with the BMP2 bead (arrowhead). **C.** BSA treated amputations at 7 DPI display strong BrdU labeling within the wound epidermis and scattered labeling of cells within the wound dermis and stump tissues. **D.** BMP2 treated amputations at 7 DPI display a cluster of BrdU labeled cells associated with the microcarrier bead (arrowhead), whereas the regenerating stump is heavily labeled (arrow). **E.** Quantification of BrdU labeling by cell counts within the connective tissue and the stump in comparable regions of BSA and BMP2 treated digits at 3 and 7 DPI. The data show BMP2 enhanced proliferation in the connective tissue at 3 DPI, and in the skeletal stump at 7 DPI (t-test, ± s.e.m, *** $p < 0.001$). **F,G:** Proliferation studies of BMP2-induced P2 regeneration in the BRE-*Gfp* transgenic reporter mouse. EdU incorporation identified proliferating cells (magenta) and BMP responsive cells were identified based on GFP immunohistochemistry (green). **F)** Double labeled cells (arrows) distal to the amputated stump and associated with the BMP2 bead are present at 3 DPI. **G)** At 1 DPI double labeled mesenchymal cells (arrows) indicative of a proliferative response to BMP2 treatment are clustered between the BMP2 bead and the amputated stump. **H–K:** In situ hybridization to identify localized changes in expression of established digit blastema marker genes. **H)** In BMP2 treated digits at 1DPI, *Msx1* transcripts are localized to cells directly associated with the BMP2 bead (arrow). **I)** In control BSA treated digits at 1 DPI, no *Msx1* expression is induced. **J)** In BMP2 treated digits at 1DPI, *Pedf* expressing cells are scattered throughout the wound mesenchyme (arrows) and do not appear directly associated with the BMP2 bead. **K)** *Pedf* expressing cells are absent in the amputation wound of control BSA treated digits at 1 DPI.

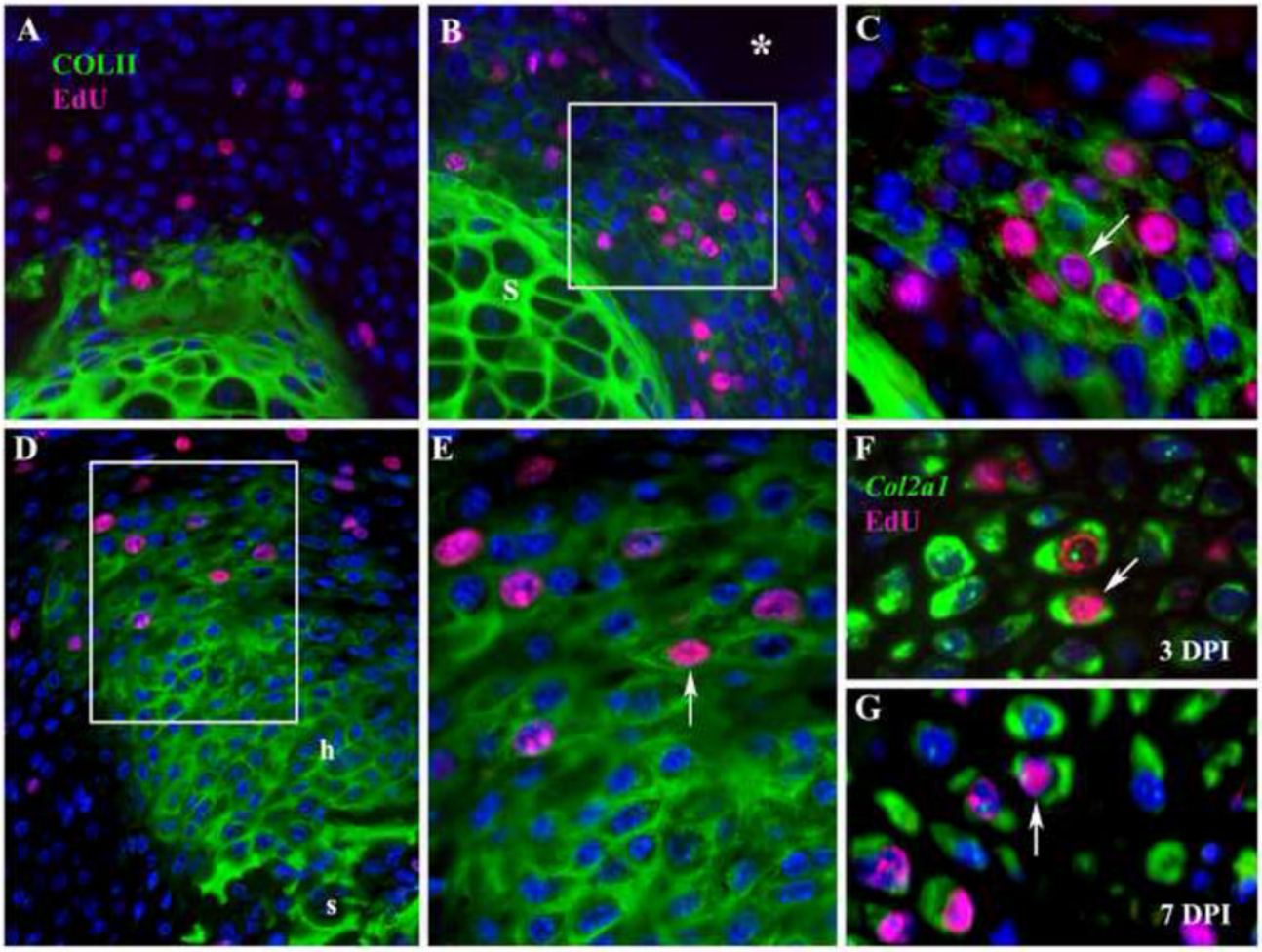

Figure 5. Chondrocyte proliferation during BMP2-induced regeneration

Distal is toward the top in all images. **A–E:** Histological sections of control BSA-treated or BMP2-treated amputated P2 elements displaying Col II immunostaining (green) to identify chondrocytes in conjunction with EdU incorporation (magenta) to identify proliferating cells. **A)** Control digit treated with BSA bead at 3 DPI displays Col II expression restricted to the amputated skeletal stump, and few proliferating cells associated with the wound healing response following amputation. No proliferating chondrocytes are found in the amputation wound. **B**) P2 amputation treated with a BMP2 bead (*) at 3 DPI displays an aggregate of cells expressing Col II and positive for the incorporation of EdU distal to the stump (box). **C**) Higher magnification of cells in **B** (box) showing individual cells (arrow) with nuclei staining positive for EdU surrounded by Col II positive staining. **D**) P2 amputation treated with a BMP2 bead (top of the figure but not shown) at 7 DPI displaying an elongate skeletal outgrowth that is positive for Col II staining and contiguous with the stump (s). Cells staining positive for EdU incorporation are localized to the distal region of the outgrowth (box). Proximal hypertrophic chondrocytes (h) are not proliferating and correlate with regions of *Col10a1* expressions (see Figure 3D). **E**) Higher magnification of cells in **D** (box) showing individual cells (arrow) that are labeled for EdU and surrounded by Col II positive staining. **F–G:** To definitively identity proliferating chondrocytes at 3 (**F**) and 7 (**G**) DPI, EdU incorporation (magenta) was used to identify proliferating cells in conjunction with FISH to identify *Col2a1*transcripts (green) localized in the cytoplasm. **F)**

At 3 DPI double labeled cells (arrow) definitively identify proliferating chondrocytes induced by BMP2. **G)** At 7 DPI double labeled cells (arrow) identify proliferating chondrocytes localized to the growing apex of the BMP2 induced regenerate.

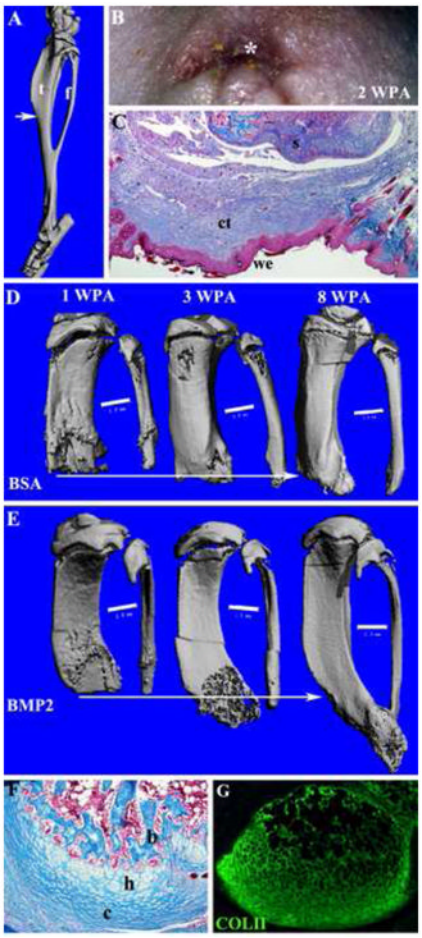

Figure 6. Regeneration response to Bmp2 after adult limb amputation

Distal is toward the bottom of all images. **A**) μCT image showing the skeleton of the mouse hind limb shank (consisting of the tibia (t) and fibula (f) that fuse distally), and the level of amputation (arrow). Simple amputation was made through the mid-shaft of the shank so as to transect both tibia and fibular proximal to the point of fusion. **B**) External examination indicated that wound closure is highly irregular due to the wound contraction response of mature skin and is complete by 2 WPA. A wound epithelium (*) is apparent by external examination. **C**) Mallory staining of histological section of an amputated limb after wound closure shows the formation of a wound epithelium (we) surrounded by mature epidermis, and underlain by connective tissue (ct) distal to the amputated skeletal stump (s). **D–E:** μCT scans of a BSA control (**D**) and a BMP2-treated limb (**E**) at 1, 3, and 8 WPA. Amputated limbs were treated after wound closure (2 WPA) by implantation of gelatin containing either BSA or BMP2 between the wound epithelium and the skeletal stump. The skeletal elements are aligned based on the proximal extent of the fibula and the arrows indicate the extent of the regenerative response. **D)** BSA control limbs showed a healing response that resulted in minor bone elongation. **E)** BMP2 treated amputations displayed organized distal bone growth resulting in skeletal elongation and distal bone fusion suggestive of a properly patterned regenerative response. Scale bars = 1 mm. **F**) Mallory staining of histological sections at 6 WPA of a BMP2 treated limb regenerate showing apical outgrowth associated with an endochondral ossification response involving distal chondrocytes (c), hypertrophic chondroctyes (h) and bone (b). **G)** Immunohistochemical staining for type II collagen of an

adjacent section to the sample shown in **F** identifies an apical localization of chondrocytes associated with the BMP2-induced regenerative response.

Following amputation in mice BMP2 induces a skeletal regenerative response

BMP2 stimulated cell proliferation and an endochondral ossification center forms

A distal growth plate like structure organizes the direction of skeletal outgrowth

BMP2 induced regeneration is specific to the level of amputation

BMP2 is a critical factor for successful limb regeneration in mammals